JOURNAL OF MATERIALS SCIENCE, 30 (1995) 1849–1853

Phase investigation in laser surface alloyed steels with TiC

S. ARIELY, M. BAMBERGER
Department of Materials Engineering, Technion Israel Institute of Technology, Haifa 32000, Israel

H. HÜGEL
IFSW, Stuttgart University, Stuttgart, Germany

P. SCHAAF
II. Physikalisches Institut der Universität Göttingen, Bunsenstraße 7-9 D-3400 Göttingen, Germany

Laser technology enables melting and alloying specimen surfaces without the substrate itself being heated, whereby surfaces with special attributes are obtained with the properties of the substrate remaining unaffected. The surfaces of Armco iron and AISI 1045 steel were laser-alloyed with TiC powder, a CO_2 laser of 2.5 kW maximum power being used. Optimal laser and powder-feed parameters were established. Particles of TiC were injected into the molten surface layer, forming a composite material, steel + TiC. The microstructures were investigated metallographically. Some of the particles had partially melted during their passage through the laser beam and had re-solidified, forming small and fine dendrites. Phase identification by X-ray diffraction revealed the presence of α-Fe, martensite, and Fe_3C phases, as well as amounts of stochiometric TiC and unknown phases. Identification of phases by TEM and diffraction of electrons revealed the presence of unknown phases, such as tetragonal TiC and (FeTi)C. Mössbauer results show ternary Fe–Ti–C phases, which can be related to the TEM and X-ray diffraction results. A correlation was found between the substrate's composition, microstructures, and the different phases present.

1. Introduction

The utilization of the laser as a means for locally heating a surface at selected sites has much expanded in recent years. The great advantage of the laser beam is the local concentration of high energy, leading to specific areas of extremely high temperatures, followed by rapid cooling of the surface. Alloying a surface is one of the important applications of laser technology and serves as a subject for a great deal of research. The possibility of changing the surface composition and structure over a wide range as well as the creation of structures and non-equilibrium phases, render the process (referred to as laser surface alloying, LSA) especially interesting and attractive. With LSA, special surface qualities can be imparted to a basic material, e.g. steel, permitting service in extreme conditions of corrosion and wear. It was the aim of the present work to characterize the structure and phases in iron-based materials laser alloyed with TiC.

2. Experimental procedure

During the experiments, TiC powder, made by Plasma Technik, with a particle-size distribution in the range 50–100 μm, was used. The composition of the powder, according to the manufacturer, was 19.55 wt % carbon (0.04 wt % free carbon), 0.065 wt % iron, 0.045 wt % nitrogen, 0.08 wt % oxygen, balanced by titanium. Working conditions were determined after preliminary experiments, in which the conditions were laser power 1750 W, powder feed rate (PFR) 0.043 $g\,s^{-1}$, and overlap between consecutive passes 50%. The laser-beam diameter was 1.2 mm, with a scanning speed of 10 $mm\,s^{-1}$. Experiments were carried out under a protective atmosphere of argon, which also served as the carrier gas. The powder was injected below the laser beam, with the direction of feed perpendicular to the specimen movement and at an angle of 45° to its surface.

2.1. Optical microscopy

The specimens were polished with SiC polishing paper to grade 600 μm, and with alumina powder to grade 0.05 μm. For etching, Nital 5% was used.

2.2. X-ray examinations

The purpose of these examinations was to study the effect of cooling rate on the formation and presence of

0022–2461 © *1995 Chapman & Hall*

the different phases. Because the cooling rate changes with distance from the treated surface, the specimen was polished and a layer 100 μm thick removed before every examination. A Bragg-Brentano diffractometer was used (reflections are only from planes parallel with the surface). The diffractometer was controlled by a PDP 11/53 computer through a Philips PW 1710 processor. The radiation was CuK_α with a graphite monochromator. Working voltage and current were 40 kV and 40 mA, respectively. Full-spectrum scanning (20°–100°) was applied. The step was 0.015°; sampling time was 1 s.

2.3. Mössbauer spectroscopy

The Mössbauer spectra were recorded at room temperature in the back-scattering geometry of conversion X-ray Mössbauer spectroscopy (CXMS) by detecting the re-emitted 6.4 keV X-rays following resonant absorption. For details of the experimental apparatus, see [1, 2]. No sample preparation was carried out after laser treatment, because CXMS enables non-destructive testing of the laser-treated surfaces [3, 4]. A constant acceleration drive and a ^{57}Co in rhodium source with an activity of about 600 MBq were used for the Mössbauer measurements. The spectra were analysed with a least squares programme [5] by superimposing Lorentzian lines. Calibration was made using α-Fe foil, and isomer shifts are always given relative to α-Fe. It is worth noting that the information range of this method is a surface layer approximately 10 μm thick [6].

2.4. Transmission electron microscopy (TEM)

TEM samples were prepared by cutting the alloyed layer from the bulk. The layer was polished to a thickness of 150 μm using diamond-coated disc. A crater 50 μm deep was created by a dimpler, using 5 μm diamond paste. A hole was made in the centre of the crater by a jet polisher using acetic acid + 5% perchloric acid as an etchant. Finally, for cleaning and improving the hole edges, the samples were polished in an ion miller at a small angle (12°) for 20–30 min.

3. Results

3.1. Optical microscopy

Figs 1 and 2 are micrographs of a cross-section of the LSA treated zone of Armco iron and AISI 1045 steel, respectively. In the both cases, TiC particles are homogeneously distributed. The surfaces are slightly rough relative to the depth of the baths. These photographs show the average depth of the melt bath to be 390 μm in case of Armco iron, and 600 μm in case of 1045 steel.

3.2. X-ray spectroscopy

X-ray spectroscopy of Armco iron shows that two phases exist throughout the laser surface-alloyed zone: α-Fe and TiC. No evidence for Fe_3C or Ti–Fe intermetallic compounds was found. From the bath centre to the bath bottom, an unknown tetragonal phase, marked as TiC′, appeared (Fig. 3). This phase was not found in the HAZ. Because its lattice parameter is very close to that of TiC, it is seen that its appearance can be correlated to the presence of the TiC.

No Fe–Ti intermetallic phases were found in the X-ray spectrum of AISI 1045 steel. The broadening of the TiC peaks can be a result of iron atoms dissolved in its lattice. In the range 400–600 μm below the

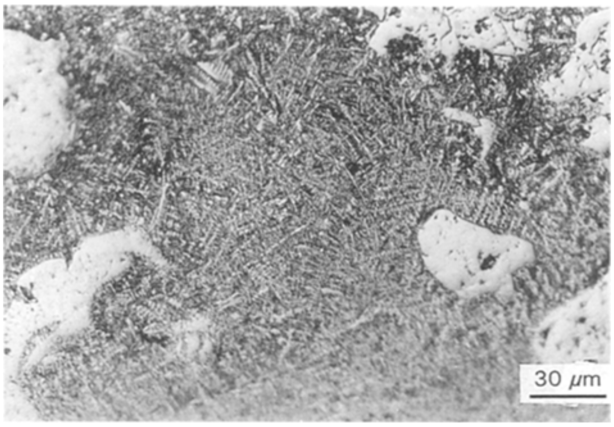

Figure 1 Photomicrograph of a cross-section of the LSA zone of Armco iron.

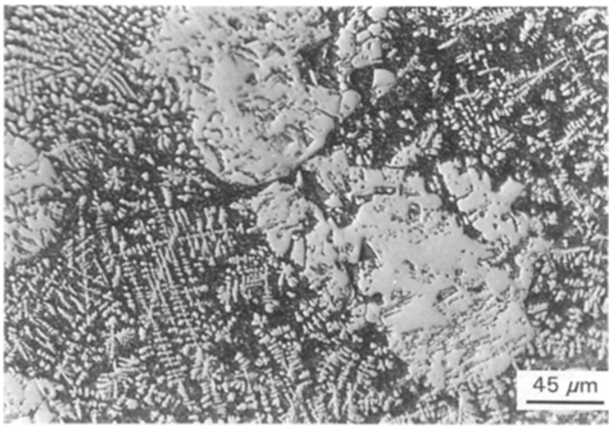

Figure 2 Photomicrograph of cross-section of the LSA zone of AISI 1045 steel.

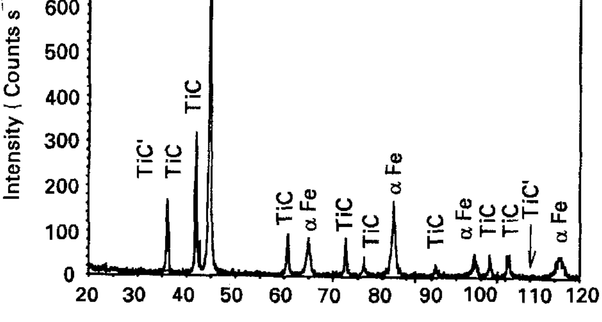

Figure 3 X-ray spectrum of the LSA zone of Armco iron.

sample surface, an unknown phase was found (Fig. 4). This phase has peaks at the same position as the unknown phase TiC′ that was identified in the Armco iron substrate. Some broadening of the iron peaks was identified at a depth of 600 μm. This could be due to martensite, which was also found in the metallography (Fig. 2). No evidence for Fe_3C was found.

3.3. Mössbauer spectroscopy

Figs 5 and 6 display the Mössbauer spectra (CXMS) of the laser-treated Armco iron, and AISI 1045. Data given for Mössbauer results in Table I are in relative area (RA) percentage, resembling only the iron atoms. Analysis of the Mössbauer spectrum of laser surface-alloyed Armco iron (Fig. 5) shows that the composition of the alloyed layer is only α-Fe with an impurity content of about 0.3 at % Ti. The impurity content in the α-Fe is calculated by a binomial distribution [7]. Thus the change compared to the untreated sample is only the small amount of titanium dissolved in the α-Fe which originates from the TiC particles in the matrix. The carbon can lead to the formation of martensite, which cannot be differentiated from the ferrite of the starting material.

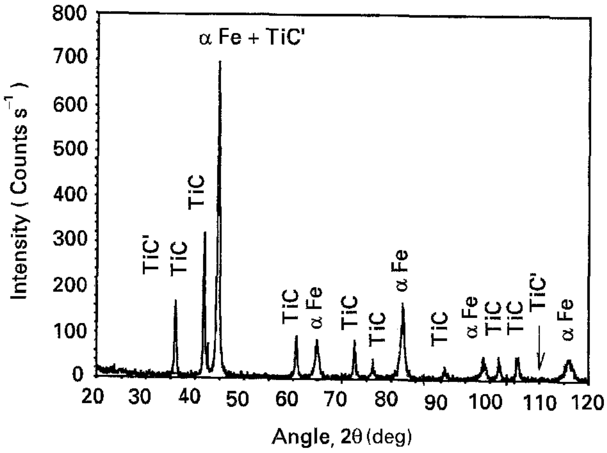

Figure 4 X-ray spectrum of the LSA zone of AISI 1045 steel.

According to Fig. 6, AISI 1045 is composed of 86 at % α-Fe with about 0.8 at % Ti dissolved, 3% Fe_3C, and 11 at % of a non-magnetic phase designated TiC″ that could be identified as f c c, because the hyperfine parameters agree well with the austenite parameters given by Bauer *et al.* [8]. The hyperfine parameters of the cementite agree well with values given in the literature [9]. Compared to the untreated sample, it seems that some of the iron from the matrix has dissolved into the TiC particles.

3.4. TEM

Fig. 7 shows a dendrite in the AISI 1045 substrate. Analysis of a diffraction pattern of this dendrite revealed a face centred tetragonal structure (f c t) with the following lattice parameters: $a = 0.411 \pm 0.004$ nm, $c = 0.519 \pm 0.006$ nm. This phase (TiC′) was

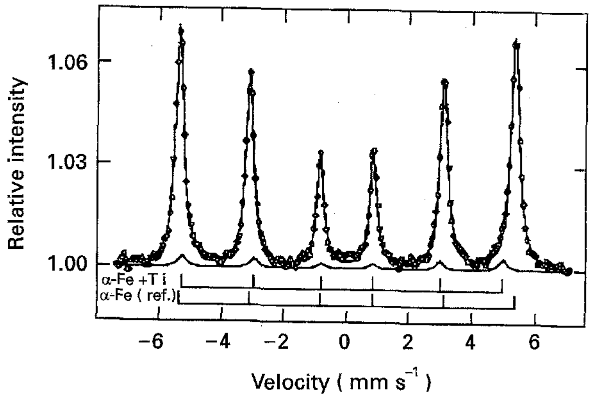

Figure 5 A Mössbauer spectrum of the LSA zone of Armco iron.

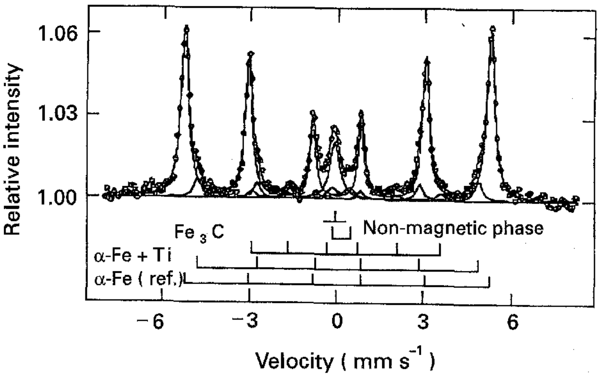

Figure 6 A Mössbauer spectrum of the LSA zone of AISI 1045 steel.

TABLE I Calculated Mössbauer hyperfine parameters

	Subspectrum[a]		IS (mm s^{-1})	QS (mm s^{-1})	H (T)	Line width (mm s^{-1})	RA (%)
Armco untreated	α-Fe	M1	0.00	0.00	33.0	0.28	100
Armco + TiC + laser	α-Fe	M1	0.00	0.00	33.3	0.32	96
	α-Fe	M2	− 0.04	0.01	31.8	0.32	4
AISI 1045	Fe_3C	C1	0.28	0.12	19.5	0.31	3
	α-Fe	M1	0.00	0.00	33.0	0.34	86
	α-Fe	M2	0.01	0.02	30.6	0.34	11
AISI 1045 + TiC + laser	γ-Fe	A1	− 0.07	–	–	0.40	8
	γ-Fe	A2	0.14	0.62	–	0.40	3
	α-Fe	M1	0.01	0.00	32.7	0.32	77
	α-Fe	M2	0.04	0.01	30.0	0.32	9
	Fe_3C	C1	0.26	0.07	20.1	0.32	3

[a] γ-Fe indicates austenite, or a cubic paramagnetic phase (Ti, Fe) C. The hyperfine parameters fit very well with austenite, the parameters of (TiFe)C are unknown. α-Fe indicates alpha iron, there is no easy possibility to distinguish between ferrite and martensite).

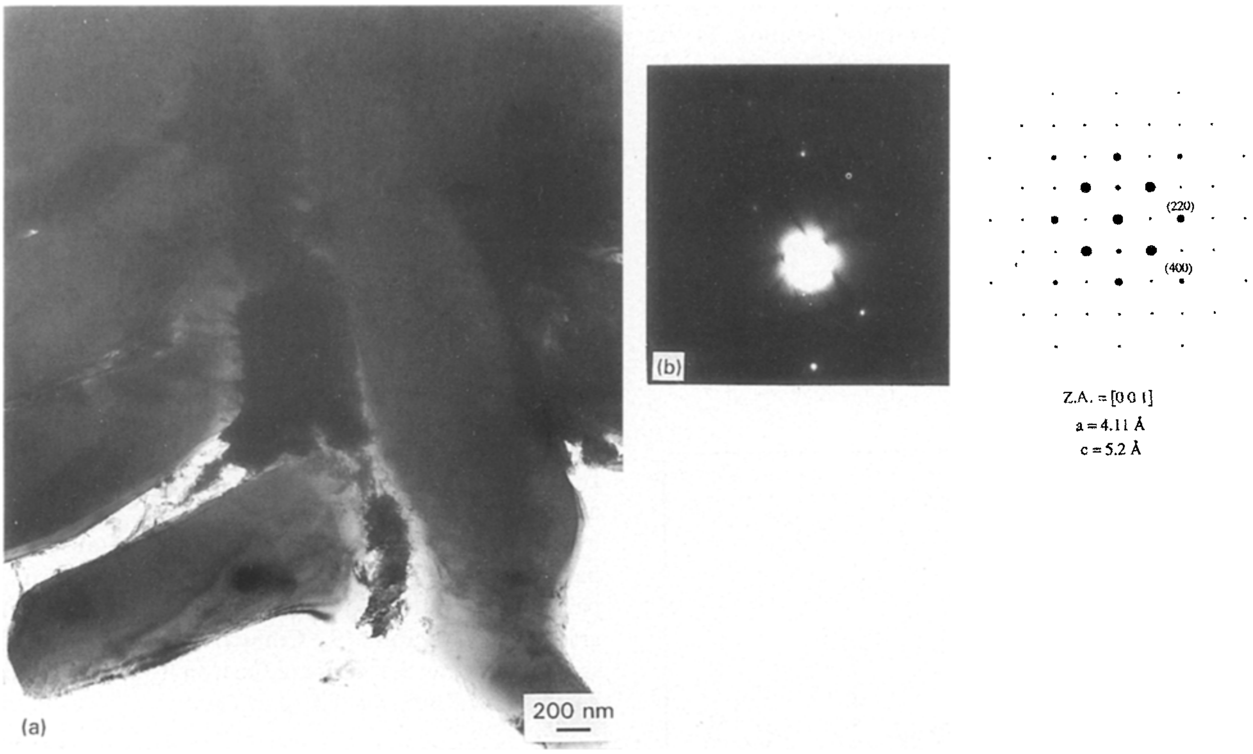

Figure 7 A bct dendrite: (a) bright-field image, (b) diffraction pattern.

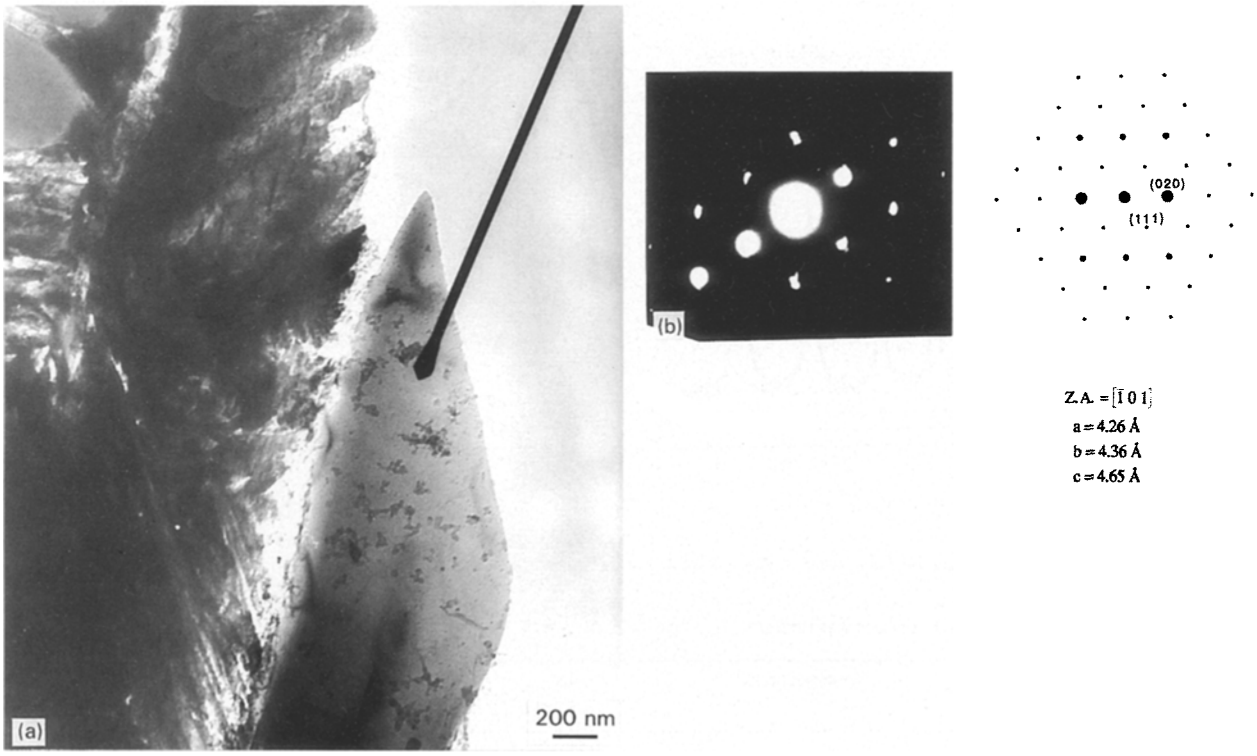

Figure 8 A face centred orthorhombic dendrite: (a) bright-field image, (b) diffraction pattern.

also found in Armco iron substrate. The structure of a second phase, designated TiC″, was identified as face centred orthorhombic with the following lattice parameters: $a = 0.426 \pm 0.002$ nm, $b = 0.436 \pm 0.001$ nm, $c = 0.465 \pm 0.0003$ nm (Fig. 8). This phase was found in AISI 1045 samples only. This phase corresponds to the non-magnetic phase identified by Mössbauer spectroscopy.

4. Discussion

The TiC dendrites clearly discernible in Figs 1 and 2 indicate that the molten layer contains iron, carbon and titanium. Because the melting point of TiC is higher than the evaporation temperature of the substrate, it can be concluded that the TiC particles melt, at least partially, during their residence inside the laser beam. This molten TiC, accompanied by the residual solid particles, entered the melt forming thereby a molten solution. The nature of this solution depends on the carbon content of the substrate, as will be explained below.

Based on Richardson diagrams [10], the solubility of TiC in iron is almost temperature independent but depends on the carbon content in the iron – varying from high solubility in pure iron at 3270 K to almost nil as the carbon content in the iron reaches 4 at %. Therefore, the carbon-free Armco iron dissolves the liquid TiC, forming a ternary solution of Fe–Ti–C. Owing to the rapid cooling, some iron atoms are trapped in the primary solidified TiC, resulting in a distorted fct structure, having the following lattice parameters: $a = 0.411$ nm, $c = 0.519$ nm as found by the TEM analysis (Fig. 7) and X-ray diffraction (Fig. 3). Because the molten AISI 1045 contains more carbon than does the Armco iron, the TiC dissolves in it only to a limited extent, whereas the excess of this carbide remains in equilibrium with this alloyed melt, i.e. the molten bath is basically composed of a molten Fe–C–TiC alloy and solid TiC. Upon cooling, a solid solution of TiC in austenite is formed [11]. Owing to the high cooling rate, a precipitation of TiC from the austenite could not result. Therefore, a super-saturated solution of TiC in austenite was formed. The unit cell of this solution is distorted, namely a face centred orthorhombic structure, having lattice parameters as follows: $a = 0.426$ nm, $b = 0.436$ nm, $c = 0.465$ nm (Fig. 8). The fcc non-magnetic phase found by the Mössbauer spectroscopy can be related to this one. The latter phase was not found in the Armco iron substrate. Because there is no excess of carbon in this substrate (a super-saturated solution of TiC in austenite), the orthorhombic phase could not be formed.

Acknowledgements

This research was partially supported by the Technion V.P.R. Fund – Tragovnik Research Fund. One of the authors (S.A.) thanks the DAAD for a scholarship, which enabled collaboration with IFSW, Stuttgart.

References

1. L. BLAES, H.-G. WAGNER, U. GONSER, J. WELSCH and J. SUTOR, *Hyperf. Interact.* **29** (1986) 1571.
2. P. SCHAAF, L. BLAES, J. WELSCH, H. JACOBY, F. AUBERTIN and U. GONSER, *ibid.* **58** (1990) 2541.
3. P. SCHAAF, V. BIEHL, M. BAMBERGER, Ph. BAUER and U. GONSER, *J. Mater. Sci.* **26** (1991) 5019.
4. P. SCHAAF, V. BIEHL, M. BAMBERGER, G. SHAFIRSTIEN, M. LANGOHR, F. MAISENHAELDER and U. GONSER, in "Proceedings of the 5th Israel Materials Engineering Conference", edited by M. Bamberger and M. Schorr (Freund Publishing House, London, 1991) pp. 451.
5. W. KUENDIG, *Nucl. Instrum. Meth.* **75** (1969) 336.
6. Ph. BAUER, O. N. C. UWAKWEH and J. M. R. GENIN, *Hyperf. Interact.* **41** (1988) 555.
7. P. SCHAAF, Ph. BAUER and U. GONSER, *Z. Metallkde* **80** (1989) 77.
8. U. GONSER, P. SCHAAF and F. AUBERTIN, *Hyperf. Interact.* **66** (1991) 95.
9. P. SCHAAF, S. WIESEN and U. GONSER, *Acta Metall.* **40** (1992) 373.
10. F. S. RICHARDSON, "Physical Chemistry of Melts in Metallurgy" (Academic Press, London, 1974).
11. H. OTHANI, T. TANAKA, M. HASEBE and T. NISHIZAWA, *CALPHAD* **12** (1988) 225.

Received 2 August 1993
and accepted 8 September 1994